



Aluminum foam made via a new method based on cold gas dynamic sprayed powders mixed through sound assisted fluidization technique

Antonio Viscusi^{a,*}, Paola Ammendola^b, Antonello Astarita^a, Federica Raganati^b, Fabio Scherillo^a, Antonino Squillace^a, Riccardo Chirone^b, Luigi Carrino^a

^a Department of Chemical, Materials and Industrial Production Engineering, University of Naples Federico II, Piazzale Tecchio 80, 80125 Naples, Italy

^b Istituto di Ricerche sulla Combustione (IRC)-CNR, Piazzale Tecchio 80, 80125 Naples, Italy



ARTICLE INFO

Article history:

Received 20 July 2015

Received in revised form

21 December 2015

Accepted 30 December 2015

Available online 4 January 2016

Keywords:

Aluminum foam

Cold spray deposition

Precursors manufacturing

Fluidization process

Fine powders

ABSTRACT

Metal foams are an interesting class of materials with very low specific weight and unusual physical, mechanical and acoustic properties due to the porous structure. In recent years several manufacturing techniques were developed. The limit of these techniques is that it is difficult, even if impossible, to manufacture precursors and then foams able to reinforce complex shaped components; this drawback, to date, limits the application of metal foams. This proof of concept paper is focused on the study of an innovative manufacturing technique able to produce complex shaped precursors. The key idea is to spray a powder mixture (made of both aluminum alloy powders as metal matrix and titanium hydride particles as foaming agent) through the cold gas dynamic spray on a free shape metallic substrate and then carry out the foaming process. A preliminary granulometric analysis was carried out to estimate the particles mean size and then sound assisted (140dB–80 Hz) fluidization process was used to achieve a homogenous and deep mixing between the fine metal powders and the blowing agent ones. In particular, two different types of mixtures with 1 wt% and 2.5 wt% of TiH₂ were investigated; moreover, air compressed as well as helium were used as CGDS carrier gas in order to ensure a higher impact velocity and a better compacting of the powders. Finally, the cross sections of manufactured solid foams were observed by means of a SEM microscope for having information about internal metallurgical phenomena as well as the distribution and morphology of foam cells. Macrographs of created porous structures showed the effectiveness of the developed innovative manufacturing process.

© 2015 Elsevier B.V. All rights reserved.

1. Introduction

Metal foams are a relatively new class of structural materials that are finding an increasing use in many applications due to their peculiar properties, such as unusual thermal and acoustic properties, high compression strength, high stiffness and good energy absorption features, as reported by [Ashby et al. \(2000\)](#). Moreover, [Khabushan et al. \(2013\)](#) found that metal foams retain some properties of the bulk metal coupled to the low weight due to the porous structure.

Metal foams of different metals are available, such as: aluminum, nickel, magnesium, lead, zinc, copper, bronze, titanium, steel and even gold. The more used in structural applications are aluminum foams that could be used as core for sandwich structures,

internal antibuckling reinforcement for thin walled structures and so on ([Lukkassen and Meidell, 2007](#)).

Aluminum foams can be manufactured through several methods that could be mainly divided in two macro groups: direct and indirect foaming methods as proposed by [Banhart \(2006\)](#). The former consists in a specially prepared molten metal containing uniformly dispersed nonmetallic particles to which gas bubbles are added to create foam; in the latter the foam is obtained starting from a solid precursor material which consists of a metallic matrix containing uniformly dispersed blowing agent particles; when this precursor is heated up at a temperature close to the melting point of the matrix the precursor expands due to the decomposition of the blowing agent and the metal foam is obtained.

Among the indirect methods, the powder metallurgy one, in which the starting materials are metal powders, is of particular interest; [Banhart \(2001\)](#) presented a detailed study on the main phases of this process. The first step consists of mixing homogeneously aluminum metal powders and titanium hydride (TiH₂) that is the blowing agent. This mixture is compacted to produce

* Corresponding author. Fax: +39 0817682362.

E-mail address: antonio.viscusi@unina.it (A. Viscusi).

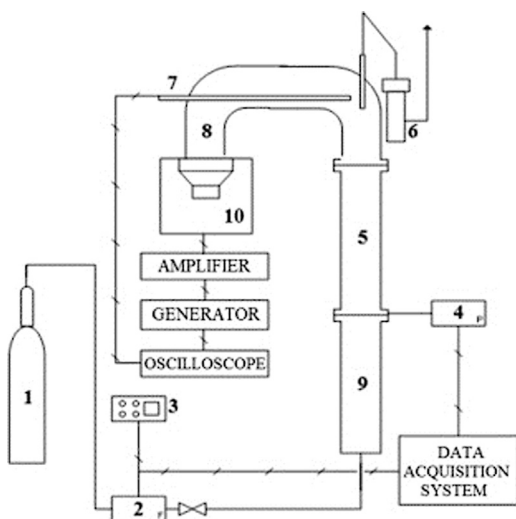


Fig. 1. Experimental apparatus: (1) nitrogen cylinder; (2) flow meter; (3) controller; (4) pressure transducer; (5) 40 mm ID fluidization column; (6) filter; (7) microphone; (8) sound guide; (9) wind-box; (10) loudspeaker.

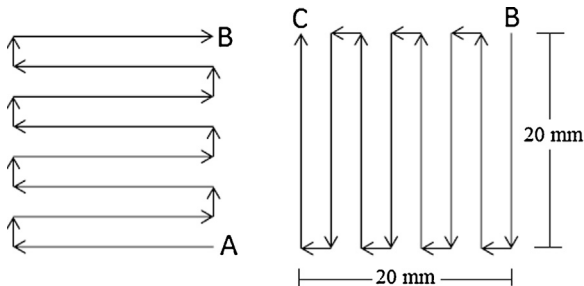


Fig. 2. Pattern performed by GDS spray gun.

Table 1
Deposition process main parameters.

| Gas used | Gas temperature [°C] | Gas pressure [bar] | Stand-off distance [mm] | Speed nozzle [mm/s] | Powder feed rate [kg/h] |
|------------|----------------------|--------------------|-------------------------|---------------------|-------------------------|
| Air/helium | 600 | 7 | 5 | 2.5 | 3.5 |

a dense “foamable precursor material” through some compaction technique (e.g. hot isostatic compression, rod extrusion, powder rolling) in order to make sure that the blowing agent is well embedded within the metal matrix and to obtain a semi-finished product without any residual porosity. In the final step, the solid precursor is placed in a furnace and heated up. The blowing agent decomposes releasing the hydrogen that induces the formation of bubbles within the metal matrix that is in incipient melting. Under these conditions, the compacted metal matrix achieves a semi-liquid viscous state and the released gas forces the melting precursor material to expand, modelling a highly porous structure. In order to ensure satisfactory foaming results, appropriately starting powders have to be chosen. To achieve an effective foaming process the melting temperature of the metal matrix and the gas decomposition temperature the blowing agent have to be very close. If the blowing agent releases gas far below the metal melting point, the metal matrix will be expanded already in the solid state, leading to formation of crack-like pores and irregularities in the final product. Conversely, if the blowing agent decomposes far above the metal melting point, the viscosity of the melt will be too low to allow the formation of a stable foam.

The most suitable materials for foaming are pure aluminum or cast alloys (e.g. AlSi7Mg and AlSi12) due to their relatively low melting points and good foamable properties. von Zeppelin et al. (2003) showed that titanium hydride (TiH_2) is the best blowing agent for these metal materials because releases the largest amount of hydrogen between 400–600 °C, which is a temperature range very close to the melting point of aluminum alloys, as reported by Matijasevic-Lux et al. Several other foaming parameters, that have to be conveniently controlled, influence the final foam quality. The most important are: powder mixing composition, particles dimensions and shape, distribution of blowing agent within the metal matrix, compaction pressure and temperature, time and temperature of foaming (which vary depending on the materials used and the size and shape of the precursor) and heating rates.

To date, the typical commercial foaming precursors are manufactured in form of extruded rods with rectangular cross section. This rigid geometry of the precursor limits the applications of these materials, indeed it is very difficult if not impossible the making of complex shaped foamed components. This paper deals with the study of an innovative manufacturing technique for the precursor that allows to overcome the above mentioned limitation. In particular it will be studied the fabrication of complex shaped precursors through the cold gas dynamic spray (CGDS) technology. The general concept is to spray a powder mixture, made of both aluminum alloy powders as metal matrix and titanium hydride particles as foaming agent, on a metallic substrate and then carry out the foaming process in order to obtain the final foamed component. The shape of the precursor can be ruled by using a complex shaped substrate or by imposing a complex trajectory at the spraying gun.

Stoltenhoff et al. (2002) found that, in CGDS, the high kinetic energy causes the impingement of the particles onto the substrate. Grujicic et al. (2004) indicated the macroscopic plastic deformation, induced by the high velocity impact, as the main bonding mechanism. Two different scenarios have been observed (Gilmore et al., 1999), depending on materials pair and particles velocity: (a) particles rebounding from the substrate (with or without erosion) or (b) particles bonding to the substrate. The velocity at which bonding is achieved is referred to as critical velocity and relies on the particle size and distribution as well as the substrate material. A more detailed discussion of this technology is reported in Astarita et al. (2013).

A key factor of this process is to obtain a homogenous and deep mixing between the metal powders and the blowing agent particles.

Classical mixing methods (such as tumbling mixers, convective mixers, high-shear mixers, including media mills and hammer mills), discussed by Kaye (1997), are suitable for large, non-cohesive particles (i.e. mean particle sizes greater than 30 μm) but not for particles smaller than 10 μm in size, always agglomerated due to strong interparticle forces as showed in Ammendola et al. (2011a,b). Alternatively, Wei et al. (2002) proposed mixing techniques for fine particles classified in wet and dry mixing. However, all these technological alternatives suffer from different disadvantages: additional steps of filtration and drying are needed in the case of wet methods and dry mixing methods generally involves the reduction of the granulometry and the damaging or contamination of the original powders.

In this respect, the use of fluidization makes it possible to overcome these problems, since it is able to handle and process large quantities of powders. Nevertheless, these fine powders fall under the Geldart's group C (<30 μm) classification according to the study of Geldart (1972), their fluidization is expected to be difficult (plug formation, channelling and agglomeration) because of high interparticle forces. Among all externally assisted fluidization techniques, Ammendola et al. (2011a,b) proved that sound assisted fluidization might be competitive in overcoming the interparticle

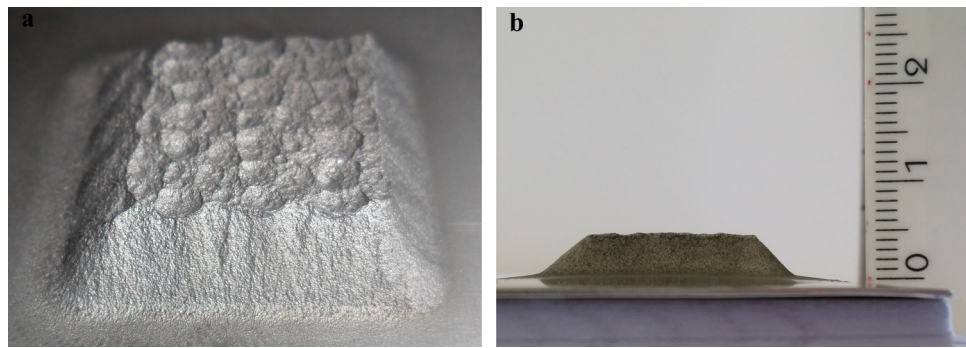


Fig. 3. Foamy solid precursor manufactured through the cold gas dynamic spray technology.

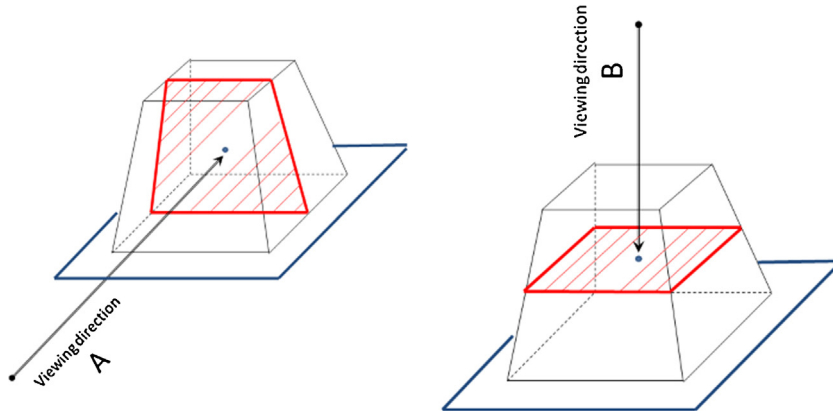


Fig. 4. Sketch of two different cross sections: orthogonal (a) and parallel (b) to the plate.

forces and achieving smooth fluidization regime since it does not affect the properties and morphology of the original particles, it is rather cheap and can be easily implemented and scaled-up. Moreover, Raganati et al. (2015) showed that the achievement of a good fluidization quality of fine particles under the effect of suitable acoustic fields (125–150 dB and 50–120 Hz) makes it possible to obtain a mixing to the scale of the primary particles (even down to nanoscale) constituting the powders in a simple and efficient way.

In our proof of concept study it has been studied the feasibility to produce complex shaped metal foam precursors through the CGDS process. The different powders, i.e. the aluminum particles and the blowing agent, were mixed through the fluidization bed technique. A preliminary experimental campaign was carried out to optimize the process parameters of the mixing process. After that, the obtained powder mix was sprayed through the CGDS process, using different carrier gas, on a metallic substrate. The obtained precursor was heated up in a furnace to obtain the desired metal foam. A detailed experimental campaign, including macroscopical observation, SEM observations and EDS analysis, was carried out on the powder mix, the precursor and the final foam.

2. Experimental procedure

2.1. Materials and equipments

The micron sized powders of aluminum alloy AlSi12 and titanium hydride TiH_2 used in this experimentation were provided by DYMET with a nominal density respectively of 2.69 g/cm^3 and 3.75 g/cm^3 . The presence of silicon within the aluminum matrix increases its fluidity and improves the foaming performances; moreover, since the weight percentage of silicon (12 wt%) is very close to eutectic composition (11.7 wt%), the melting point of the

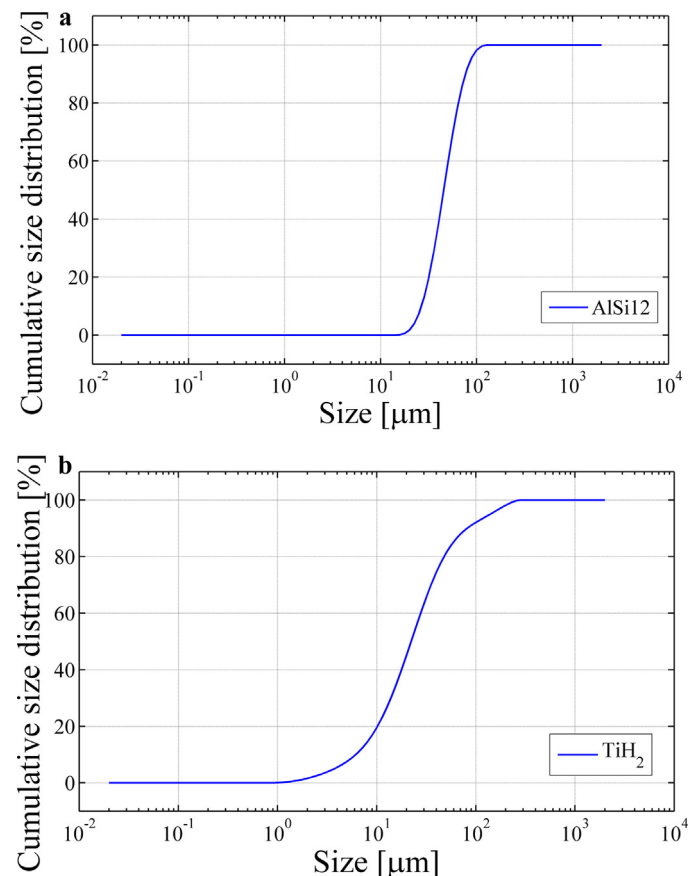


Fig. 5. Cumulative size distribution of AlSi12 (a) and TiH_2 (b) powders.

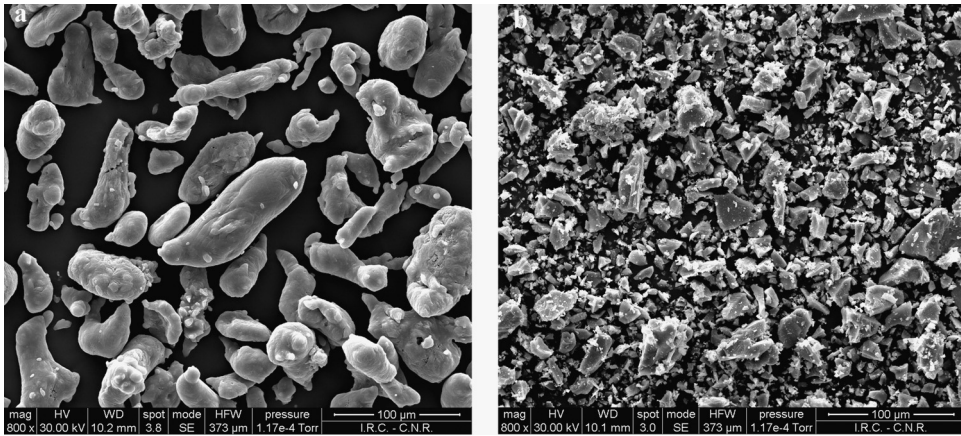


Fig. 6. SEM images of AlSi12 (a) and TiH₂ (b) powders at magnification 800X.

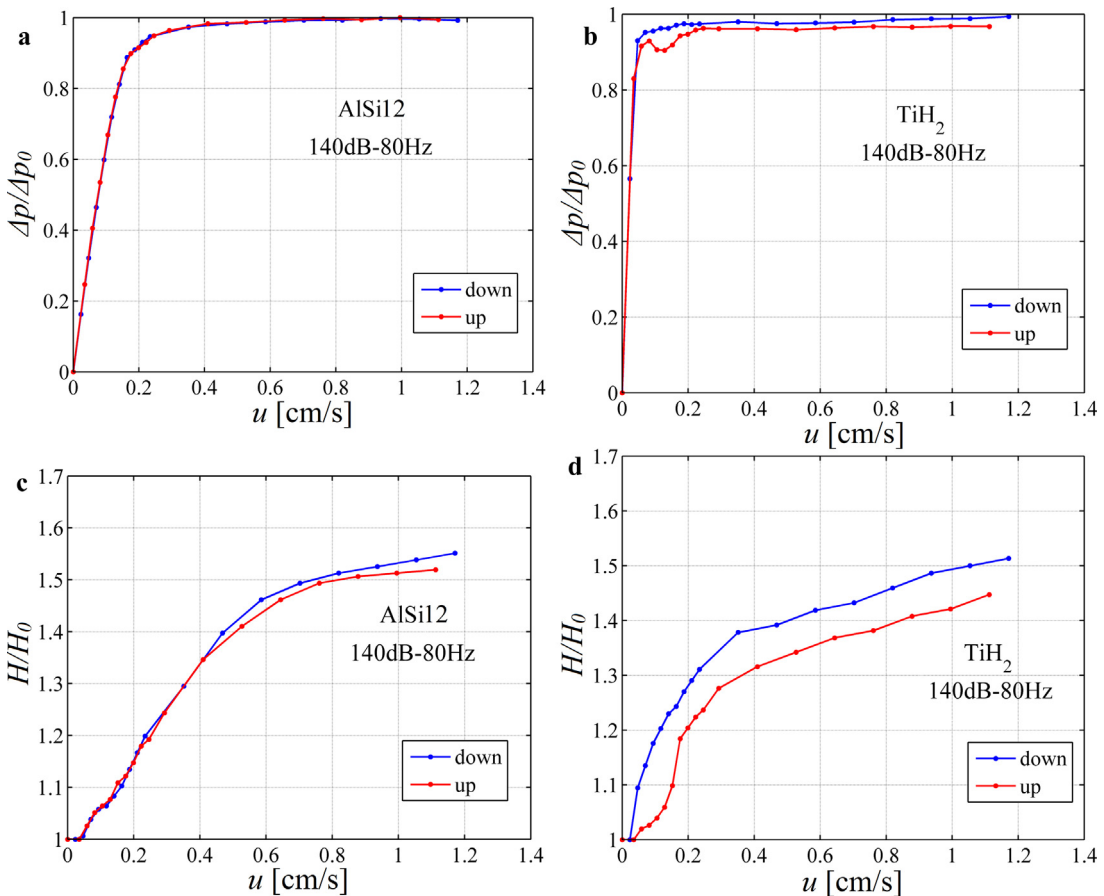


Fig. 7. Dimensionless pressure drop ($\Delta p/\Delta p_0$) and bed expansion (H/H_0) as functions of superficial gas velocity during sound assisted fluidization with the application of acoustic fields (140dB–80 Hz) for AlSi12 ((a), (c)) and TiH₂ ((b), (d)) powders.

alloy is relatively low (573–585 °C) and similar to the decomposition temperature of the blowing agent used. The particle mean size and the cumulative size distribution of both powders were evaluated using a laser granulometer (Master-sizer 2000 Malvern Instruments) after the dispersion of the powders in water under mechanical agitation of the suspension and with the application of ultrasound. A SEM microscope (SEM HITACHI TM3000) was also used to observe specimens of particles of both powders. The fluidization and mixing tests of these cohesive fine powders were performed by the experimental apparatus schematically reported in Fig. 1. It consists of a laboratory scale fluidization column (40 mm

ID and 500 mm high), made of Plexiglas, equipped with a porous plate gas distributor, a 300 mm high wind-box filled by Pyrex rings to maximize the uniformity of the gas flow rate entering the column, a pressure transducer installed at 5 mm above the gas distributor to measure the pressure drop of the gas across the bed. The acoustic field is introduced inside the column through a sound wave guide located at the top of the column. Ammendola and Chirone (2010) designed the sound wave guide to prevent the elutriated powders from dirtying the loudspeaker. The sound-generation system is made of a digital signal generator to obtain an electric sine wave of specified frequency whose signal is ampli-

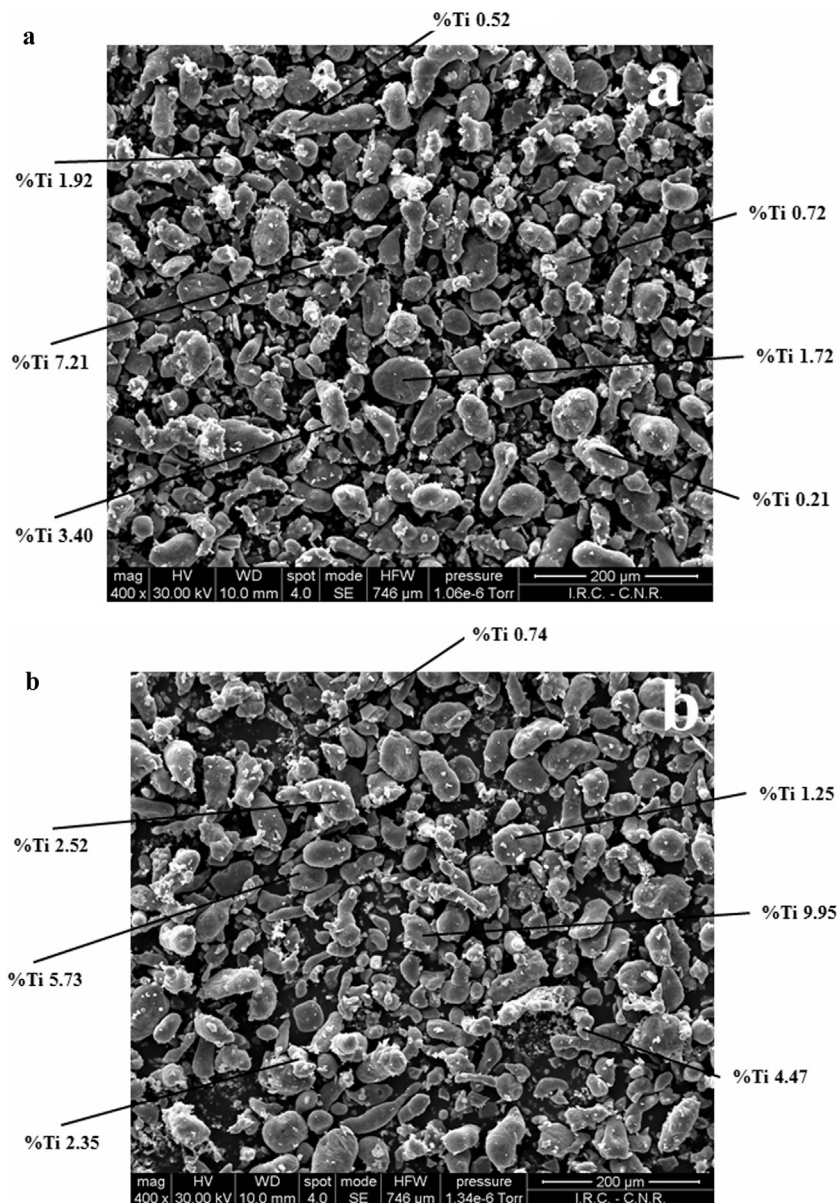


Fig. 8. SEM images and EDS analysis of the powders aggregates. Sample taken after 2 min during the (a) A and (b) B mixing tests.

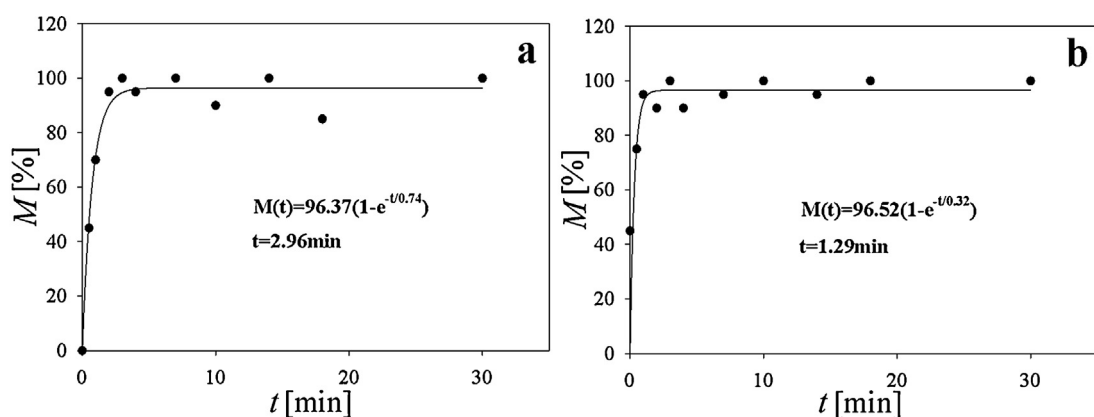


Fig. 9. Time-dependence of the aggregates mixing degree for (a) A and (b) B mixing tests.

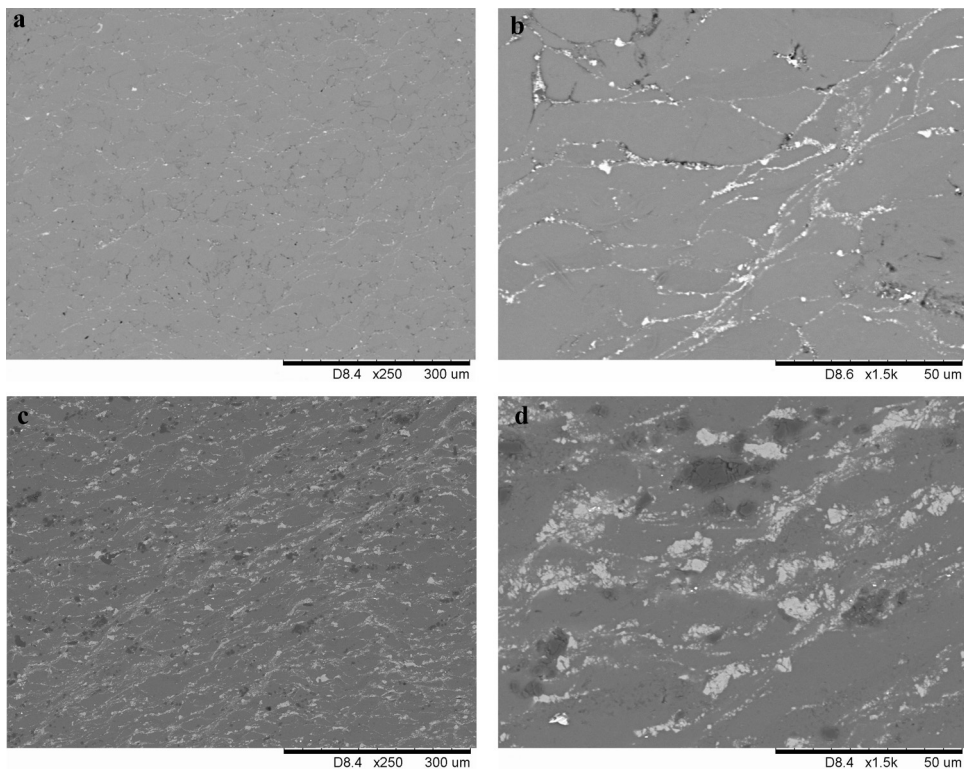


Fig. 10. SEM images of solid precursors manufactured by means of CGDS technology: $S_{1,h}$ at magnification 250X (a) and 1500X (b), $S_{2,5,a}$ at magnification 250X (c) and 1500X (d).

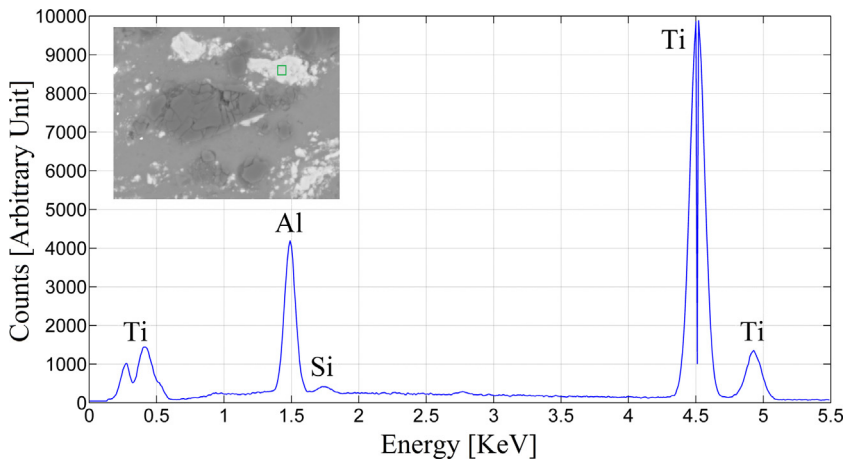


Fig. 11. X-rays spectrum of titanium hydride particles.

fied by means of a power audio amplifier rated up to 40 W. The signal is, then, sent to an 8 W woofer loudspeaker placed downstream the sound wave guide. Pure dry nitrogen from a compressed tank is used as fluidizing gas. The flow rate of gas is controlled by a mass flow controller (Brooks). All the tests were carried out at room temperature and ambient pressure conditions. Both the preliminary fluidization/mixing tests and the preparation of the final $AlSi12-TiH_2$ mixtures to be used to produce the metal foam precursors were performed in this experimental apparatus.

Valid binary mixture specimens of each sample were observed through SEM microscope to appreciate the mixing degree achieved.

Low pressure cold spray facility was used for spraying the powders constituting the foamable precursor. It is a compact light weighted gas dynamic spray machine with a GDS spray gun, two powder feeders and a control unit. Control unit includes fluid pres-

sure and fluid temperature control and powder feeders switch with powder feed rate regulators.

In this research activity the deposition process was automated by means of a pantograph which is numerically controlled remotely; in fact the cold-spray nozzle was attached to a robot (*HIGH-Z S-400/T CNC-Technik*) to allow for control and repeatability of the coating deposition. The spraying parameters such as fluid temperature and fluid pressure, stand-off distance (the distance between the substrate and the nozzle) and horizontal speed nozzle across the substrate are summarized in Table 1; they were chosen after a preliminary experimental campaign that is not discussed in this paper for the sake of brevity.

Both compressed air and helium were used as carrier gas; the latter was employed in order to bring down internal oxidation phe-

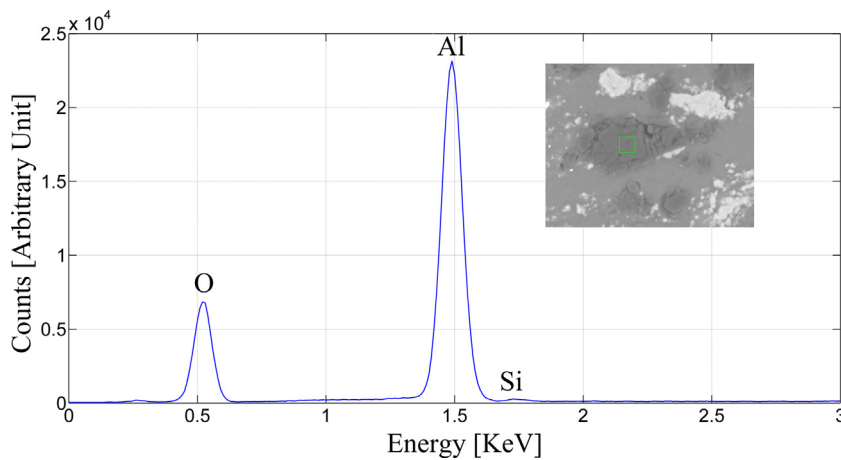


Fig. 12. X-rays spectrum of alumina particles.

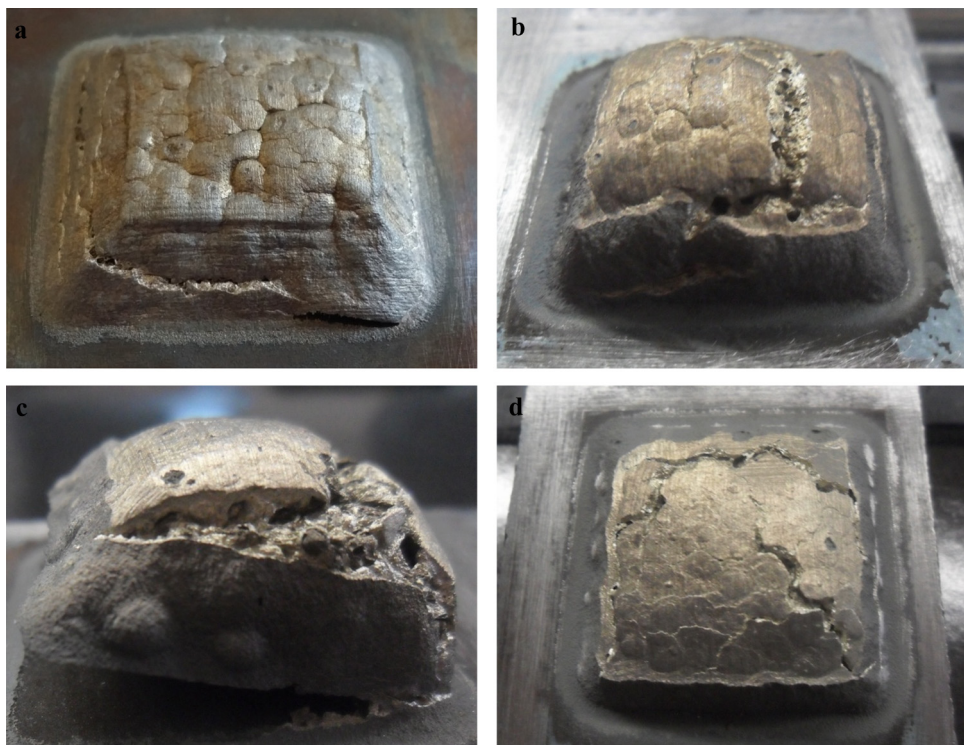


Fig. 13. Cold sprayed foamed precursors: 1 wt% of TiH_2 -Air (a) and Helium (b) 2.5 wt% of TiH_2 -Air (c) and Helium (d).

nomena, ensure a higher impact velocity of the particles and a better compacting of the powders.

2.2. Preliminary fluidization and mixing tests of AlSi12 and TiH_2

Fluidization tests were carried out with an initial bed of 150 g for both the powders. Pressure drop ($\Delta P/\Delta P_0$) and bed expansion (H/H_0) curves were obtained both in ordinary and sound assisted conditions by decreasing (DOWN) and increasing (UP) the superficial gas velocity, ΔP being the actual pressure drop across the bed, ΔP_0 the pressure drop equal to buoyant weight of particles per unit area of bed, H the actual bed height and H_0 the initial bed height under fixed bed conditions. Then, the minimum fluidization velocity, u_{mf} , was calculated from the pressure drop curves by means of a graphic procedure described in Ammendola and Chirone (2010). The parameters of the acoustic field (intensity = 140 dB; frequency = 80 Hz) were set according to the results

obtained from previous experimental campaign providing a good fluidization quality for a wide range of materials (Ammendola et al., 2011a,b).

Mixing tests between AlSi12 and TiH_2 were performed with the application of the above-mentioned acoustic field in order to evaluate the mixing kinetics and, therefore, the time necessary to achieve the desired mixture composition. Experiments were carried loading 150 g of the binary mixture loading the AlSi12 powder and then the TiH_2 one. Each test was carried out for about 120 min. The superficial gas velocity was fixed at 1.2 cm/s (i.e. which is more than seven times the minimum fluidization velocity of the powders under these sound-assisted conditions), thus ensuring the fluidization of the entire bed. Two different types of mixtures with 1 wt% (A mixing test) and 2.5 wt% (B mixing test) of TiH_2 were tested. The former is a mixture with a composition close to the conventional produced precursors (0.8 wt% TiH_2), the latter is richer of TiH_2 in

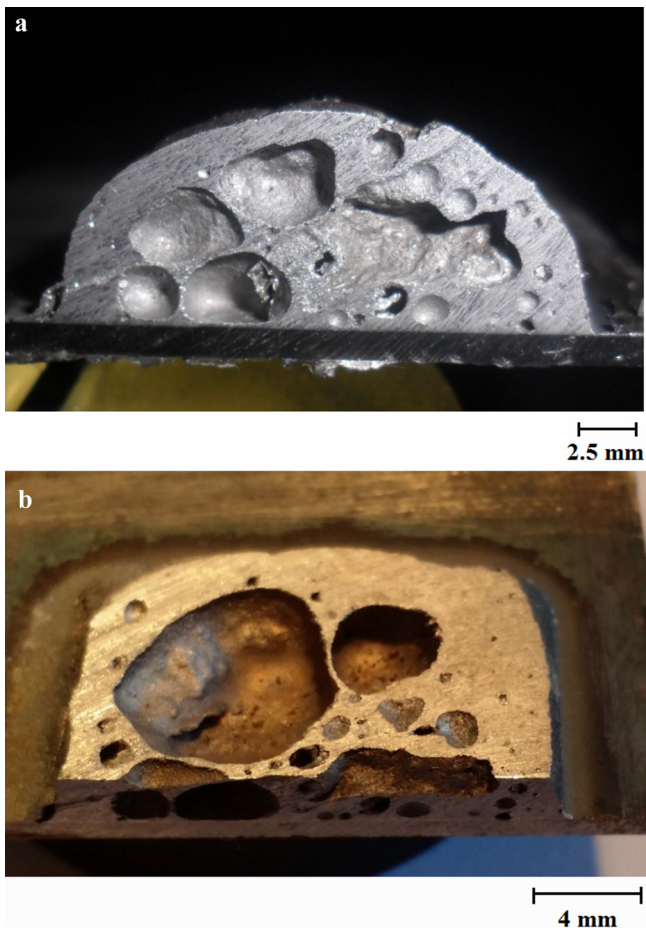


Fig. 14. Cross sections of $S_{1,h}$ foamed precursor: orthogonal (a) and parallel (b) to the substrate.

order to balance the low efficiency deposition of CGDS technique according to the study presented by Hodder et al. (2014).

Cross section macrographs of the specimen $S_{1,a}$ and $S_{2.5,h}$ that showed an ineffective foaming are showed in Fig. 16

During experiments samples of the fluidized materials were taken at different times (0.5, 1, 2, 3, 4, 7, 10, 14, 18, 30, 60, 120 min) by means of a non-destructive sampling procedure widely presented in Ammendola and Chirone (2010). These samples were then analyzed to determine the chemical composition of aggregates by SEM analysis carried out with a Philips XL30 SEM equipped with an EDAX instrument for micro-analysis. In particular, 50 aggregates were randomly chosen and analyzed for each sample. The time dependence of the mixing degree, its asymptotic value and the mixing characteristic time were evaluated.

On the basis of all preliminary fluidization/mixing tests the final AlSi12-TiH₂ mixtures to be used to produce the metal foam precursors were prepared following the same procedure described for the mixing tests (superficial gas velocity of 1.2 cm/s and acoustic field of 140dB–80 Hz). The mixtures preparation lasted about 15 min, i.e. more than five times the obtained mixing characteristic time.

2.3. Manufacturing of solid precursors

Each powder mixture was sprayed on a 0.5 mm stainless steel thin plate; moreover, in order to achieve a homogeneously material deposition, square plan form foaming precursors with the size of 20 × 20 mm were manufactured according to the scheme reported in Fig. 2.

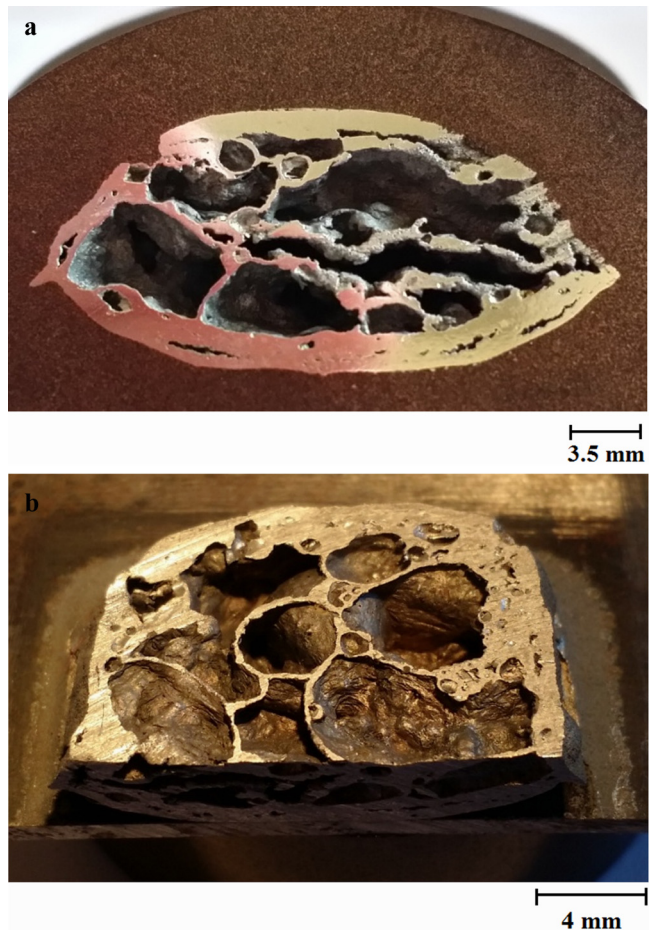


Fig. 15. Cross sections of $S_{2.5,a}$ foamed precursor: orthogonal (a) and parallel (b) to the substrate.

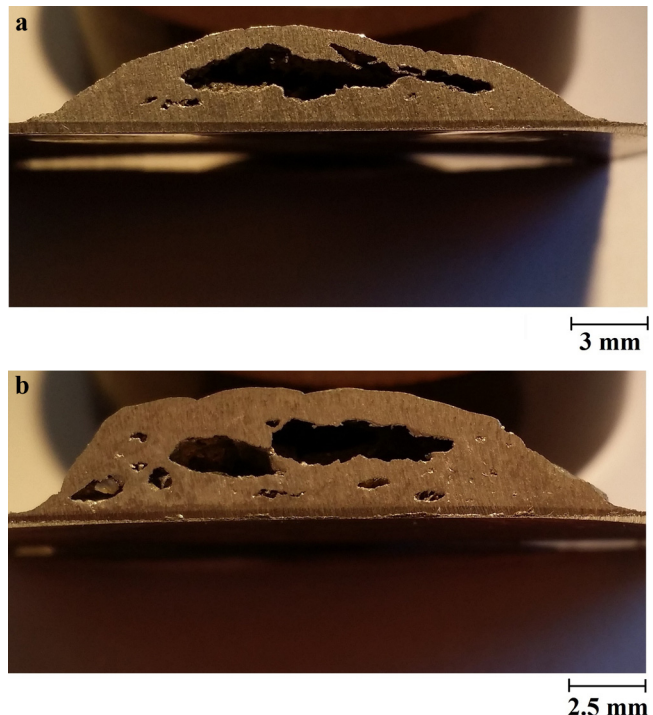


Fig. 16. Cross sections of $S_{1,a}$ (a) and $S_{2.5,h}$ (b) foamed precursors.

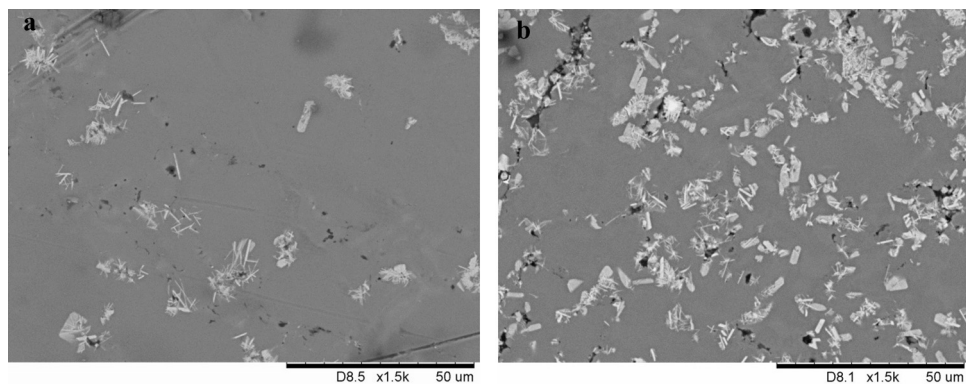


Fig. 17. SEM images of a cell wall of S_{1,h} (a) and S_{2,5,a} (b) foamed precursors.

Table 2

Test matrix of solid precursors obtained through the cold gas dynamic spray technology.

| | Air | Helium |
|-----------------------------|--------------------|--------------------|
| 1 wt% of TiH ₂ | S _{1,a} | S _{1,h} |
| 2.5 wt% of TiH ₂ | S _{2,5,a} | S _{2,5,h} |

Spray nozzle, starting from A, tracks the pattern (a) with a stand-off distance of 5 mm, as declared in [Table 1](#); after that, the pattern (b) was tracked. In order to take into account the stand-off reduction due to the material deposited, an increment of 3 mm was imposed to reach again a stand-off of 5 mm.

This deposition procedure twice are performed, producing a final thickness sprayed precursors of approximately 5 mm. Through the materials and equipments above, it was obtained the full test matrix reported in [Table 2](#).

As an example, it is shown in [Fig. 3\(a\)](#) foamable solid precursor manufactured through the cold gas dynamic spray technology to appreciate its peculiar geometrical features. It is evident in [Fig. 3\(b\)](#) that its thickness is very close to 5 mm, like typical commercial foaming precursors.

After the deposition process of solid precursors, the cross section of these coatings was observed through the SEM microscope in order to evaluate the distribution of the blowing agent into the aluminum matrix or the presence of pores and internal defects.

2.4. Foaming process

The foaming process was carried out in a preheated furnace at 650 °C, the foaming time was estimated according to preliminary experimental tests; in fact the time needed for full expansion depends on temperature and the size of the precursor and ranges from a few seconds to several minutes. In this activity a foaming time of 7–9 minutes was considered; afterwards each sample has been taken out from the furnace and cooled to the room temperature. In order to appreciate the cell distribution and morphology within the foam, the foamed specimens were cut in two different cross sections ([Fig. 4](#)), orthogonal and parallel to the same substrate, and then observed through the SEM microscope due to theirs anisotropic behavior. All the specimens for metallographic observations were cut, mounted and prepared according to the international ASTM standards.

3. Discussion and results

3.1. AlSi12 and TiH₂ powders characterization

[Fig. 5](#) shows the results of the granulometric analysis, in terms of powders cumulative size distribution, for both the AlSi12 and TiH₂ powders. The Sauter mean diameter (defined as the diameter of a

sphere having the same volume/surface area ratio as a particle of interest) of AlSi12 and TiH₂ is 41.9 and 12.9 μm, respectively. In particular, TiH₂ is characterized by a broader particle size distribution (2–200 μm) than AlSi12 (20–100 μm).

High magnification SEM images of both the powders are reported in [Fig. 6](#). The irregular shape of the powders is evident, and it could be also highlighted that the AlSi12 particles have a mean diameter significantly larger than the blowing agent particles. According to the Geldart's classification both AlSi12 and TiH₂ are fine cohesive powders, meaning that their fluidization is expected to be very difficult due to their tendency to form aggregates.

3.2. Fluidization and mixing results of AlSi12 and TiH₂ powders

In ordinary conditions (i.e. without the application of any acoustic field) a poor fluidization quality was obtained: the powders were not able to reach a full fluidized state, in fact pressure drop curves do not approach the unity and bed expansion ones are quite irregular. This phenomenon is more evident for titanium hydride powder because it has stronger cohesive character with respect to AlSi12 due to its smaller particle size (its mean particle diameter, 12.9 μm, is about four times smaller than that of aluminum alloy mean, 41.9 μm).

The application of an acoustic field is required to achieve a proper fluidization regime, improving the fluidization quality. The energy introduced in the bed through the acoustic waves is able to break-up large aggregates into smaller ones promoting the fluidization of the entire bed; in fact, it can be seen ([Fig. 7](#)) that the application of acoustic fields results in more regular pressure drop and bed expansion curves for both powders. Moreover, [Fig. 7](#) shows that the bed reaches a full fluidized state, since dimensionless pressure drop ($\Delta p/\Delta p_0$) curves approach the unity. In particular, the minimum fluidization velocities, u_{mf} , calculated from the pressure drop curves are 0.17 and 0.05 cm/s for AlSi12 and TiH₂ powders, respectively, according to their different particle mean size.

The efficiency of mixing between the two powders, promoted by the application of a suitable acoustic field, has been verified. Samples of the fluidized materials were taken from the upper part of the bed at different times according to the ad-hoc non-destructive sampling procedure described in the experimental section. The different samples were, then, analyzed by SEM/EDS analysis in order to determine the aggregates chemical composition. On the basis of the relative amount of TiH₂ and AlSi12, the Ti weight composition corresponds to 0.96 and 2.4% for A and B tests, respectively. These values are the theoretical limit corresponding to a complete mixing both at the global scale (average composition of the bed) and at the local scale (average composition of aggregates).

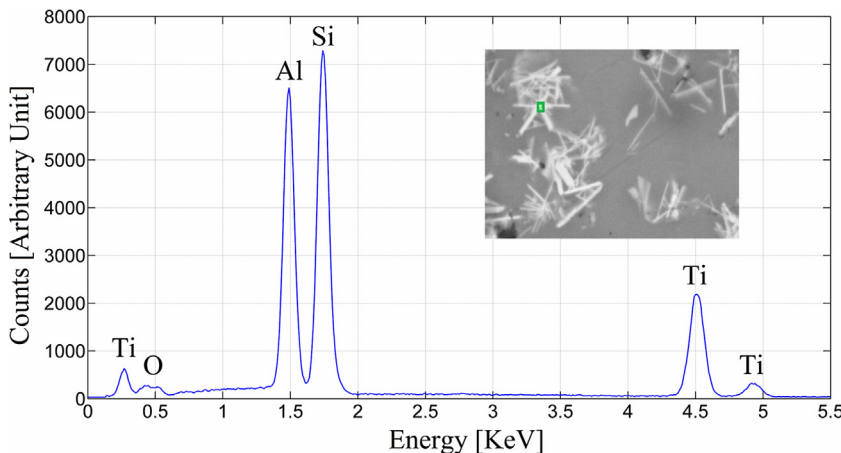


Fig. 18. X-rays spectrum of Ti-Si intermetallic compounds.

Table 3

Results of cold sprayed solid precursors: highlighted in bold the samples showing the best results.

| | Air | | | Helium | | |
|-----------------------------|------------|---------------------------|------------------------------|------------|---------------------------|------------------------------|
| | Mass [g] | Volume [mm ³] | Density [g/mm ³] | Mass [g] | Volume [mm ³] | Density [g/mm ³] |
| 1 wt% of TiH ₂ | 2.9 | 1679.6 | 1.7 × 10 ⁻³ | 4.1 | 1817.1 | 2.3 × 10⁻³ |
| 2.5 wt% of TiH ₂ | 4.7 | 1801.1 | 2.6 × 10⁻³ | 2.7 | 1306.6 | 2.1 × 10 ⁻³ |

Fig. 8 reports the SEM images and EDS analysis of powders aggregates taken during A and B tests at 2 min after the application of sound. All the aggregates are formed of both TiH₂ and AlSi12, thus meaning that the mixing process takes place at the local scale, namely not only between aggregates made of only one powder but also inside aggregates leading to the formation of hybrid aggregates. This evidence is due to an actual dynamic evolution of aggregates (due to a continuous break-up and re-aggregation mechanism) typical of the sound-assisted fluidization process (Ammendola and Chirone, 2010). As a matter of fact, aggregates are mixed even after 1 min of sound-assisted fluidization and their composition varies over a wide range.

The EDS data were elaborated to evaluate the time-dependence of the aggregates mixing degree $M(t)$ for A, and B tests (Fig. 9), where M at a fixed time is defined as the ratio between the number of aggregates whose Ti composition differs from the theoretical one less than 5% and the total number of aggregates analyzed at time t . Each data series was fitted with an exponential rise-to-maximum law $M(t) = a(1 - \exp(-t/b))$.

The analysis of these curves shows that, whatever the relative amount of the two powders, the mixing quality is very high: the asymptotic value of $M(t)$ is larger than 96% and the characteristic time is lower than 3 min, i.e. less than 3 min are needed for more than 96% of aggregates to be efficiently mixed.

3.3. Microscopic analysis of the precursor

Table 3 reports the mass, volume and density measurements for all the precursors produced. It can clearly notice that an effective deposition, in terms of mass and volume of the precursor, was achieved in two deposition conditions: (1 wt% of TiH₂-Helium ($S_{1,h}$) and 2.5 wt% of TiH₂-Air ($S_{2.5,a}$)). Under these conditions the estimated density of the precursors was very close to the aluminum one (2.69 g/cm³).

High magnification SEM micrographs of the $S_{1,h}$ and $S_{2.5,a}$ precursors were showed in Fig. 10. Both the precursors appear quite dense and free of porosity, with the foaming agent particles (lighter zones in Fig. 10) homogeneously dispersed within the aluminum-

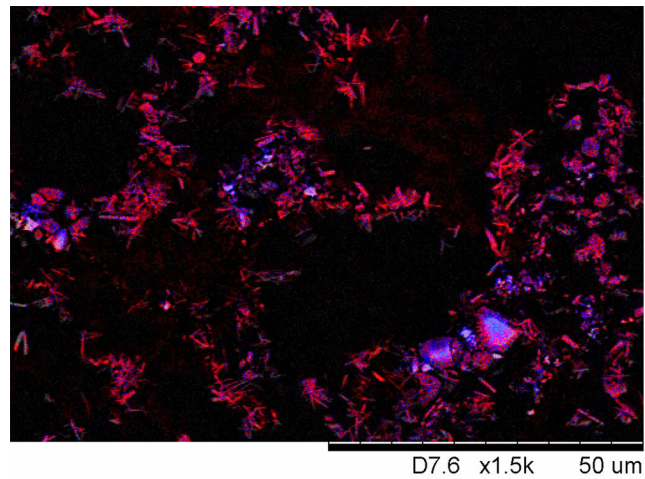


Fig. 19. Map elements of a not foamed zone of $S_{2.5,a}$ post foaming precursor: titanium (blue)-silicon (red) precipitates. (For interpretation of the references to colour in this figure legend, the reader is referred to the web version of this article).

Table 4

Numerical data of X-rays spectrum of titanium hydride particles.

| Element | Weight% | Atomic% |
|----------|---------|---------|
| Titanium | 86.118 | 77.780 |
| Aluminum | 13.269 | 21.275 |
| Silicon | 0.613 | 0.945 |

silicon matrix (grey zone in Fig. 10); moreover, a stratification of TiH₂ particles, related to technology employed, can be identified. EDS analysis confirmed the presence of alumina (Al₂O₃) particles within the precursor (dark grey in figures), which was produced during the deposition process. This latter phenomenon is less prominent in Fig. 10(a) and (b) because inert helium, that avoids oxidation phenomena of the particles to be sprayed, was employed as carrier gas. Figs. 11 and 12, coupled respectively with

Table 5

Numerical data of X-rays spectrum of alumina particles.

| Element | Weight% | Atomic% |
|----------|---------|---------|
| Aluminum | 48.443 | 36.147 |
| Silicon | 1.406 | 0.743 |
| Oxygen | 50.151 | 63.110 |

Table 6

Foaming data results: the subscripts *pf* and *bf* mean post and before foaming conditions, respectively. The two lowest relative densities were highlighted.

| | Air | | Helium | |
|------------------------------------|----------------------|----------------------|----------------------|----------------------|
| | $S_{1,a}$ | $S_{2.5,a}$ | $S_{1,h}$ | $S_{2.5,h}$ |
| $V_{pf} [\text{mm}^3]$ | 2630.7 | 4778.1 | 3998.6 | 2504.3 |
| $\rho_{pf} [\text{g/mm}^3]$ | 1.1×10^{-3} | 0.9×10^{-3} | 1.0×10^{-3} | 1.1×10^{-3} |
| $\rho_{rel} [\rho_{pf}/\rho_{bf}]$ | 0.65 | 0.35 | 0.43 | 0.52 |

Tables 4 and 5, show the results obtained from the above EDS analysis.

3.4. Foaming results

Fig. 13 shows macrographs of the aluminum foams obtained starting from the above described precursors. It can observe, as expected, an effective swelling of the material due to the decomposition reaction of the blowing agent; furthermore, the release of hydrogen gas during the foaming results in a detaching of the precursor from the substrate. Foaming data results are summarized in Table 6.

A better expansion can be observed in specimens $S_{1,h}$ and $S_{2.5,a}$ in Fig. 13, with a considerable increasing of volume and a very low relative density, 0.43 and 0.35, respectively. The reason is that when compressed air is used as carrier gas, efficiency deposition of CGDS technique is low and a high number of titanium hydride particles does not bind to the substrate; therefore a mixture with 2.5 wt%, that is slightly higher than the one used in conventional precursors, of blowing agent is necessary to achieve a good foaming expansion and to overcome the low deposition efficiency. Conversely, the efficiency deposition of the process is higher when inert helium is used as carrier gas and a mixture with 2.5 wt% of TiH_2 leads to poor foaming results, due to the large amount of blowing agent. Therefore, under these conditions, a percentage of 1 wt% of TiH_2 ensures better foaming results.

After the foaming process the $S_{1,h}$ and $S_{2.5,a}$ samples were sectioned and observed as described in Fig. 4. Optical images are showed in Figs. 14 and 15.

It is possible to observe a typical cellular structure with a pronounced anisotropy of the cells, during the foaming process the bubbles seems to grow along a preferential direction (Figs. 14 and 15).

This phenomenon is related to the CGDS technology which involves a flattening of the particles in the direction orthogonal to the deposition. In fact, during foaming process, bubbles tend to expand in the plane parallel to the substrate more easily than in the normal one.

The cross sections of the foams show some typical collapse mechanisms of metal foams. The presence of large cells suggest the occurrence of coalescence (namely the phenomenon occurring when two or more cells merge to form one larger) phenomena among several bubbles of little dimension. In the bottom, furthermore, the phenomenon of drainage occurs; i.e. molten metal flows downward from the cell walls due to gravity. Finally, the collapse is observed when no more hydrogen gas is released and the foam begins to decay after reaching the maximum expansion. Lázaro et al. (2013) proved that these phenomena occur when the dwell

Table 7

Numerical data of X-rays spectrum of Ti–Si intermetallic compounds.

| Element | Weight% | Atomic% |
|----------|---------|---------|
| Titanium | 30.679 | 19.285 |
| Aluminum | 24.485 | 27.324 |
| Silicon | 38.266 | 41.025 |
| Oxygen | 6.570 | 12.366 |

time in the furnace is too high. In fact, in this first proof of concept experimentation, the foaming process was carried out in the same conditions for all specimens.

Looking at Fig. 16 it is possible to see that a kind of expansion occurred but it is not possible to recognize a cellular structure, so the foaming process is ineffective for these specimens.

Metallurgical analysis were also carried out on cell walls and in the not foamed zones. Fig. 17 shows SEM images of a cell wall of both examined samples ($S_{1,h}$ and $S_{2.5,a}$ foamed precursors).

Due to the foaming process, aluminum alloy metal matrix becomes depleted of silicon, which is no longer present in eutectic percentage. This phenomenon promotes the formation of Ti–Si intermetallic compounds with a dendritic morphology (as confirmed by EDS analysis shown in Fig. 18 and Table 7); this phenomenon is more prominent in not fully foamed zones and can affects the process itself and the final product.

Fig. 19 reports an EDS map of the distribution of the different chemical elements that clearly shows these titanium (blue)-silicon (red) precipitates within nearly pure aluminum metal matrix.

4. Conclusions

On the basis of the experimental results presented and discussed in the previous sections the following considerations could be drawn:

- Under optimized processing conditions (i.e. with the application of acoustic fields, 140dB–80 Hz) the fluidization process was proved to be a technique to mix aluminum and titanium hydride powders of different size. After the mixing process an uniform dispersion of TiH_2 particles within the AlSi12 powders was obtained.
- The cold spray deposition technique allowed to manufacture the precursors for the foaming process. In particular when helium was adopted as carrier gas a better deposition efficiency was obtained. In fact when using helium the lower percentage of TiH_2 (i.e. 1 wt%) showed the better results, on the contrary when using air a higher percentage of TiH_2 (i.e. 2.5 wt%) must be adopted to compensate for the lower deposition efficiency of the spraying process.
- Under optimal spraying conditions, in terms of both process parameters and powder mixing quality, compact precursors with a homogeneous dispersion of TiH_2 powders within the aluminum metal matrix were obtained.
- The foams obtained from the specimens $S_{1,h}$ and $S_{2.5,a}$ (1 wt% of TiH_2 -helium and 2.5 wt% of TiH_2 -air, respectively) showed a well developed cellular structure after the foaming process. The cells were slightly anisotropic, this due to the stratification induced by the spraying process. Moreover, some intermetallic particles were observed due to the depletion of aluminum matrix during the foaming process, that leads to the formation of these Ti–Si intermetallic compounds.
- Summarizing, the CGDS process under optimal conditions, was proved to be an effective technique in producing aluminum precursors for metal foams.

Acknowledgement

The authors acknowledge Mr. Luciano Cortese for SEM/EDS analyses to evaluate the mixing efficiency.

References

- Ammendola, P., Chirone, R., 2010. Aeration and mixing behaviours of nano-sized powders under sound vibration. *Powder Tech.* 201, 49–56.
- Ammendola, P., Chirone, R., Raganati, F., 2011a. Fluidization of binary mixtures of nanoparticles under the effect of acoustic fields. *Adv. Powder Technol.* 22, 174–183.
- Ammendola, P., Chirone, R., Raganati, F., 2011b. Effect of mixture composition, nanoparticle density and sound intensity on mixing quality of nanopowders. *Chem. Eng. Process. Process Intensif.* 50, 885–891.
- Ashby, M.F., Evans, A.G., Fleck, N.A., Gibson, L.J., Hutchinson, J.W., Wadley, H.N.G., 2000. *Metal Foams: A Design Guide*. Butterworth-Heinemann.
- Astarita, A., Durante, M., Langella, A., Montuori, M., Squillace, A., 2013. Mechanical characterization of low-pressure cold-sprayed metal coatings on aluminium. *Surf. Interface Anal.* 45, 1530–1535.
- Banhart, J., 2001. Manufacture, characterisation and application of cellular metals and metal foams. *Prog. Mater. Sci.* 46, 559–632.
- Banhart, J., 2006. Metal foams: production and stability. *Adv. Eng. Mater.* 8 (9), 781–794.
- Geldart, D., 1972. The effect of particle size and size distribution on the behaviour of gas-fluidised beds. *Powder Tech.* 6, 201–215.
- Gilmore, D.L., Dykhuizen, R.C., Neiser, R.A., Roemer, T.J., Smith, M.F., 1999. Particle velocity and deposition efficiency in the cold spray process. *J. Therm. Spray Technol.* 8 (4), 576–582.
- Grujicic, M., Zhao, C.L., DeRosset, W.S., Helfritch, D., 2004. Adiabatic shear instability based mechanism for particles/substrate bonding in the cold-gas dynamic-spray process. *Mater. Des.* 25, 681–688.
- Hodder, K.J., Nychka, J.A., McDonald, A.G., 2014. Comparison of 10 µm and 20 nm Al-Al₂O₃ metal matrix composite coatings fabricated by low-pressure cold gas dynamic spraying. *J. Therm. Spray Technol.* 23 (5), 839–848.
- Kaye, B.H., 1997. *Powder Mixing*. Chapman & Hall, pp. 19–35, 77–131.
- Khabushan, J.K., Bonabi, S.B., Aghbagh, F.M., Khabushan, A.K., 2013. A study of fabricating and compressive properties of cellular Al-Si (355.0) foam using TiH₂. *Mater. Des.* 55, 792–797.
- Lázaro, J., Laguna-Gutiérrez, E., Solórzano, E., Rodríguez-Pérez, M.A., 2013. Effect of microstructural anisotropy of PM precursors on the characteristic expansion of aluminum foams. *Metall. Mater. Trans. B* 44, 984–991.
- Lukkassen, D., Meidell, A., 2007. *Advanced Materials and Structures and their Fabrication Processes*. Narvik University College, HiN, pp. 116–118.
- Raganati, F., Ammendola, P., Chirone, R., 2015. Role of acoustic fields in promoting the gas–solid contact in a fluidized bed of fine particles. *KONA Powder Part. J.* 32, 23–40.
- Stoltenhoff, T., Kreye, H., Richter, H.J., 2002. An analysis of the cold spray process and its coatings. *J. Therm. Spray Technol.* 11 (4), 542–550.
- von Zeppelin, F., Hirscher, M., Stanzick, H., Banhart, J., 2003. Desorption of hydrogen from blowing agents used for foaming metals. *Compos. Sci. Technol.* 63, 2293–2300.
- Wei, D., Dave, R., Pfeffer, R., 2002. Mixing and characterization of nanosized powders: an assessment of different techniques. *J. Nanopart. Res.* 4, 21–41.